Research article

NMR IN BIOMEDICINE

Received: 29 November 2013, Revised: 13 January 2014, Accepted: 17 January 2014, Published online in Wiley Online Library: 9 March 2014

(wileyonlinelibrary.com) DOI: 10.1002/nbm.3092

Exercising calf muscle T_2^* changes correlate with pH, PCr recovery and maximum oxidative phosphorylation

Albrecht Ingo Schmid[a,b]*, Kiril Schewzow[a,b], Georg Bernd Fiedler[a,b], Sigrun Goluch[a,b], Elmar Laistler[a,b], Michael Wolzt[c], Ewald Moser[a,b] and Martin Meyerspeer[a,b]

Skeletal muscle metabolism is impaired in disorders like diabetes mellitus or peripheral vascular disease. The skeletal muscle echo planar imaging (EPI) signal (S_{EPI}) and its relation to energy metabolism are still debated.

Localised 31P MRS and S_{EPI} data from gastrocnemius medialis of 19 healthy subjects were combined in one scanning session to study direct relationships between phosphocreatine (PCr), pH kinetics and parameters of T_2^* time courses. Dynamic spectroscopy (semi-LASER) and EPI were performed immediately before, during and after 5 min of plantar flexions. Data were acquired in a 7 T MR scanner equipped with a custom-built ergometer and a dedicated $^{31}P/^{1}H$ radio frequency (RF) coil array.

Using a form-fitted multi-channel $^{31}P/^{1}H$ coil array resulted in high signal-to-noise ratio (SNR). PCr and pH in the gastrocnemius medialis muscle were quantified from each ^{31}P spectrum, acquired every 6 s. During exercise, $S_{EPI}(t)$ was found to be a linear function of tissue pH(t) (cross-correlation $r = -0.85 \pm 0.07$). Strong Pearson's correlations were observed between post exercise time-to-peak (TTP) of S_{EPI} and (a) the time constant of PCr recovery $\tau_{PCr\ recovery}$ ($r = 0.89$, $p < 10^{-6}$), (b) maximum oxidative phosphorylation using the linear model, $Q_{max,\ lin}$ ($r = 0.65$, $p = 0.002$), the adenosine-diphosphate-driven model, $Q_{max,ADP}$ ($r = 0.73$, $p = 0.0002$) and (c) end exercise pH ($r = 0.60$, $p = 0.005$).

Based on combined accurately localised 31P MRS and T_2^* weighted MRI, both with high temporal resolution, strong correlations of the skeletal muscle S_{EPI} during exercise and tissue pH time courses and of post exercise S_{EPI} and parameters of energy metabolism were observed. In conclusion, a tight coupling between skeletal muscle metabolic activity and tissue T_2^* signal weighting, probably induced by osmotically driven water shift, exists and can be measured non-invasively, using NMR at 7 T. © 2014 The Authors. *NMR in Biomedicine* published by John Wiley & Sons, Ltd.

Keywords: ^{31}P MRS; skeletal muscle; T_2^*; exercise; plantar flexion; energy metabolism; pH; 7 Tesla

INTRODUCTION

Skeletal muscle is the main contributor to energy expenditure of the human body and an important target of insulin, which stimulates myocellular nutrient uptake and storage (1). Studying the metabolic and vascular state of skeletal muscle can therefore play a key role in aiding better understanding of diseases like diabetes mellitus and its complications, peripheral artery disease or other cardio-vascular disorders. In this study, dynamic ^{31}P MRS was used to investigate exercising skeletal muscle energy metabolism combined with T_2^* weighted ^{1}H MRI, sensitive to tissue water shift and blood oxygenation (2,3), within one measurement session.

Numerous studies have been published using ^{31}P MRS techniques, ranging from a more technical focus to basic physiology and various diseases in humans (2,4). In particular, time-resolved *in vivo* concentrations of phosphorylated creatine (PCr), inorganic phosphate (P_i) and intracellular pH can be quantified. From their kinetics, the adenosine triphosphate (ATP) turnover can be inferred

* *Correspondence to: Dr A. I. Schmid, Medical University of Vienna, Center for Medical Physics and Biomedical Engineering, MR Centre of Excellence, Lazarettgasse 14, 1090 Wien, Austria.*
E-mail: albrecht.schmid@meduniwien.ac.at

a *A. I. Schmid, K. Schewzow, G. B. Fiedler, S. Goluch, E. Laistler, E. Moser, M. Meyerspeer*
Center for Medical Physics and Biomedical Engineering, Medical University of Vienna, Währinger Gürtel 18-20, 1090 Wien, Austria

b *A. I. Schmid, K. Schewzow, G. B. Fiedler, S. Goluch, E. Laistler, E. Moser, M. Meyerspeer*
MR Centre of Excellence, Medical University of Vienna, Lazarettgasee 14, 1090 Wien, Austria

c *M. Wolzt*
Department of Clinical Pharmacology, Medical University of Vienna, Währinger Gürtel 18-20, 1090 Wien, Austria

Abbreviations used: *ATP, adenosine triphosphate; ADP, adenosine diphosphate; BOLD, blood oxygen level dependent; CSI, chemical shift imaging; EPI, echo planar imaging; MVC, maximum voluntary contraction; PCr, phosphocreatine; P_i, inorganic phosphate; RF, radio frequency; ROI, region of interest; Q_{max}, maximum oxidative phosphorylation; semi-LASER, localisation with classical excitation and adiabatic selective refocusing (a single-shot MR spectroscopy sequence relatively insensitive to B_1); SNR, signal-to-noise ratio; S_{EPI}, EPI signal intensity; TTP, time to peak; VOI, volume of interest.*

and maximal mitochondrial output Q_{max} (5–7) can be derived from PCr recovery rate constants after exercise-induced depletion.

This information is very specific, as ATP turnover is acquired dynamically *in situ*, i.e. directly in the working muscle during and after exercise.

Especially during recovery from exercise or ischaemia, ^{31}P MRS data are often interpreted as a measure of mitochondrial capacity or fitness. The underlying assumption is that potential systemic limitations — cardiac output, arterial and venous flow, tissue perfusion and oxygenation — can be ignored and that mitochondrial function is the rate-limiting factor. By combining ^{31}P MRS and near-infrared spectroscopy data in patients with peripheral vascular disease, it has been shown that this is not necessarily the case (8). Also, in healthy volunteers (9) and in different types of myositis, capillary perfusion was suggested to limit recovery from exercise (10).

Compared with high-energy phosphate concentrations obtained from ^{31}P spectra, alterations in echo planar imaging (EPI) signal intensity (S_{EPI}) are not so straightforward to interpret (3,11,12). Several effects influence the skeletal muscle EPI signal simultaneously, such as changes in T_2, and T_2^*, which result from alterations in capillary blood oxygenation, volume and most prominently tissue water distribution. Osmotic effects of altered metabolite and acid-base equilibrium also contribute to alterations in water content. Both higher water content and blood oxygenation increase T_2^* (13,12). As summarised by Prompers *et al*. (2), increased metabolic activity such as PCr breakdown into P_i and Cr or glycogenolysis into lactate results in accumulation of metabolites to which the cell membrane is relatively impermeable. The accompanying osmotic pressure leads to water shift between intra- and extracellular compartments and hence to observable T_2 changes, first reported by Fleckenstein *et al*. (14). On top of this, effects of altered tissue volume and the blood oxygen level dependent (BOLD) effect contribute to the observed signal intensity. Unfortunately, the relative contributions are not easy to separate and depend on fibre type, exercise duration and intensity (15,16,3,17). When using relatively long T_R, T_1 and flow effects can be neglected.

Recently, a model for a more quantitative analysis of skeletal muscle EPI signal (S_{EPI}) data was developed (18). A motivation for the present study is to contribute to the interpretation of the muscle S_{EPI} effect by exploring the combination of this model with recent improvements of specificity and sensitivity in localised ^{31}P MRS at ultra-high field. Even though the model was designed for ischemia-reperfusion S_{EPI} data initially, the time courses in exercise recovery share the same features.

In this study, we combined mechanical force measurements, localised ^{31}P spectroscopy and functional ^{1}H MRI within the same region of interest and high temporal resolution. The benefits of high SNR from 7 T static magnetic field (19) and a dedicated form-fitted multi-channel radio frequency (RF) coil (20) allow for acquisition of dynamic muscle-specific MRS data using accurate localisation with classical excitation and adiabatic selective refocusing (semi-LASER) (21,22) at high temporal resolution (i.e. 6 s). The SNR with this set-up is comparable to that using 3 T non-localised ^{31}P spectroscopy with a single loop coil (23) and allows us to focus on one particular muscle only. With B_1 (RF field) localisation only, some signal from other muscles will always contribute, thereby resulting in a mixture of at least two metabolic pools. In particular, the P_i resonance is known to broaden or even split, possibly due to physiological (24,25) or partial volume effects (26). Also, the line width is typically lower in smaller voxels. Given sufficient SNR (23), accurately localised spectroscopy can therefore improve data interpretation by reducing ambiguity. In EPI, in addition to the SNR gain by higher magnetic field strengths, the higher sensitivity of the MRI signal to susceptibility at 7 T and generally shorter T_2 increase the contrast in T_2^* weighted S_{EPI} (27,19).

EXPERIMENTAL

The protocol was approved by the local ethics committee and was in accordance with the Declaration of Helsinki. 21 healthy subjects were recruited; one female was measured twice.

Data acquisition

Subjects (10 men, 11 women, age 20–30 years, body mass index (BMI) 18.7–25.2 kg/m^2) were measured on a 7 T scanner (Magnetom 7 T, Siemens Medical Solutions, Erlangen Germany) employing a custom-built ergometer, designed for plantar flexions inside the scanner. An in-house built ^{31}P/^{1}H transceive coil, shaped to a half cylinder of diameter $d = 14$ cm form-fitted to the human calf, was used for imaging and spectroscopy. The ^{1}H channel consisted of two array elements and the ^{31}P channel of three (20). The lengths of the ^{31}P and ^{1}H elements were $l = 10$ cm and $l = 12.5$ cm, respectively.

After instructing and positioning the subject in the ergometer, which was placed on the bed of the MR scanner, maximum voluntary contraction force (MVC) was measured by repeatedly pushing against the blocked ergometer pedal. The resistance of the pedal was then set to 30 % of individual MVC.

First, axial gradient echo images (30 slices, field of view = 160 mm × 160 mm, slice thickness = 4.8 mm, matrix size = 256 × 256, $T_E = 4.5$ ms, $T_R = 570$ ms) were acquired as anatomical reference and used for region of interest (ROI) placement.

The exercise experiment started 30 min after arrival on site and consisted of two blocks. Each block started with necessary adjustments, including shimming, and required approximately 15 min. The delay also served for standardisation, i.e. volunteers were in a relaxed, resting state. This was followed by 2 min of baseline measurements at rest, 5 min exercise and 20 min recovery for EPI imaging or 7 min of recovery for localised ^{31}P MRS. S_{EPI} data were always acquired before the ^{31}P measurements. This design was chosen because the S_{EPI} signal can remain elevated for up to 25 min before returning to pre exercise levels (28,18,29). It allowed for a stable S_{EPI} baseline and for ~ 40 min of recovery before the ^{31}P MRS acquisition during the second exercise block. PCr and pH values, on the other hand, are known to return to baseline much faster.

Echo planar imaging (measurement block one) was performed with a repetition time of $T_R = 6$ s, $T_E \approx 20$ ms and 270 repetitions, lasting for 27 min. One 6 mm slice with a matrix size of 128 × 128 and an in-plane voxel size between 1.25 and 1.5 mm — depending on calf cross-section — was acquired. Localised ^{31}P spectra (measurement block two) were acquired using a single-voxel semi-LASER sequence (21), selecting the maximum double-oblique cuboid volume that fitted into each subject's medial gastrocnemius muscle. It was verified on multiple slices that contributions from the adjacent soleus muscle were not included. The average volume was 57 × 19 × 36 mm^3 (or 35.7 ± 7.6 cm^3), while the T_R was 6 s. The RF power was adjusted by varying the system reference voltage to maximise signal from the volume of interest (VOI), as described in (21). The shortest possible echo time was selected, limited by pulse duration and transmit voltage, i.e. $T_E = 24$ ms in most subjects,

25 ms in four subjects and 26 ms in one subject. Data were acquired for 14 min.

Between minutes 2 and 7 of each block, the volunteers were asked to perform two plantar flexions every $T_R = 6$ s during the inactive periods of the pulse sequence, acoustically triggered by gradient sound.

Data processing and quantification

The EPI signal was quantified from a ROI in gastrocnemius medialis, excluding large vessels, drawn on the image averaged over the recovery period. The ROIs were applied to the image time series and the signals were integrated for each time point. The resulting time courses were normalised to the median of the first 20 scans, i.e. the baseline during rest. Muscle cross-sectional areas were calculated from the ROIs. Image registration of the EPI data was investigated but not included in the analysis, because misalignments, when present, were too small so that the registration would not improve data quality.

The S_{EPI} signal as a function of time (t) during recovery was then fitted to a model

$$\begin{aligned} f(t) &= g(t) + s(t) + l_0 + l_1(t - t_0) \\ g(t) &= g_0(t - t_0)^{g_1}\, e^{g_2(t-t_0)} \\ s(t) &= s_0 \frac{1}{1 + e^{-s_1(t-t_0-t_1)}} \end{aligned} \quad [1]$$

described previously (18). From the fit results, post exercise time to peak (TTP) and peak amplitudes were derived.

Single-shot ^{31}P MRS spectra were processed and fitted (AMARES (30)) using jMRUI (31). Resulting PCr and P_i signal intensities and pH values were exported. Where absolute values of concentrations were required, values for the resting-state concentrations of [PCr] = 34 mmol/l and [ATP] = 8.2 mmol/l cellular water were used (32). At rest, 85 % of total creatine was assumed to be phosphorylated (33). The PCr recovery time constant ($\tau_{PCr\ recovery}$) and the concentration of depleted PCr at the end of exercise ([PCr]$_{\ end\ exercise}$) were determined by fitting a single exponential function to the PCr signals.

From these results, the initial PCr recovery rate

$$V_{PCr} = \Delta[PCr]/\tau, \quad [2]$$

end exercise ADP concentration

$$[ADP] = \frac{[Cr][ATP]}{[H^+][PCr]K_{eq}}, \quad [3]$$

maximum oxidative phosphorylation according to the linear model

$$Q_{max,\,lin} = [PCr]_{rest}/\tau, \quad [4]$$

and the ADP-driven model

$$Q_{max,\,ADP} = V_{PCr} \cdot \left(1 + \frac{K_m}{[ADP]_{end\ exercise}}\right) \quad [5]$$

were derived, as described in (5).

Force and angular position of the pedal were recorded using built-in sensors. The mechanical work was calculated as the time integral over the product of force, angle and lever for each pedal push.

Measured data are given as mean ± standard deviation, if not explicitly stated otherwise. $S_{EPI}(t)$ and pH(t) were compared by cross-correlation analysis with a linear model

$$S_{EPI}(t) = a \cdot pH(t) + b \quad [6]$$

from $t = 2$ min to $t = 8$ min (i.e. after 1 min of recovery) of the experiment.

RESULTS

Muscle energetics derived from localised ^{31}P spectroscopy and parameters of S_{EPI}, measured in two consecutive blocks of a single session, are summarised in Table 1, together with demographic information. 19 subjects completed all measurements successfully, but data quality of two subjects was insufficient due to motion artefacts. High SNR (PCr_{rest}: 82 ± 19) resulting from a 7 T scanner and a dedicated, form-fitted RF coil array allowed for tissue-specific placement of the volume of interest in the gastrocnemius medialis. The boundaries between muscle groups were clearly visible in echo-planar images and large vessels were easily identified for exclusion from ROIs. An EPI difference image (recovery - baseline) and a time-series stack of ^{31}P spectra are shown in Figure 1. For this purpose, the difference of 30 averaged images during recovery and 20 from baseline were registered to the underlying gradient-echo image (Fig. 1a). The model applied to quantify S_{EPI} time courses was found to describe the signal well, with a R^2 of the fit of 0.92 ± 0.13.

During exercise, which started after 2 min of image acquisition at rest, S_{EPI} dropped rapidly to a minimum within less than 1 min, before increasing gradually over the remaining exercise period (Fig. 2a). In contrast, pH (Fig. 2b) increased initially before starting to drop. The evolution of $S_{EPI}(t)$ was very similar to the

Table 1. Summary of subject demographics and measured data

	Mean ± standard deviation
Subjects	8 m / 11 f[a]
Age	25.4 ± 2.7 y
BMI	21.5 ± 1.8 kg/m^2
$\tau_{PCr\ recovery}$	83 ± 72 s
$\tau_{P_i\ recovery}$	60 ± 45 s
PCr depletion	81 ± 15 %
$PCr_{end\ exercise}$	6.62 ± 5.08 mmol/l
pH_{rest}	7.02 ± 0.03
$pH_{end\ exercise}$	6.75 ± 0.23
TTP S_{EPI}	178 ± 109 s
Peak post exercise S_{EPI}	1.24 ± 0.14
ΔS_{EPI}	0.16 ± 0.08
Work / plantar flexion	10.0 ± 2.8 J
Work / area	1.4 ± 0.5 J/cm^2
Power	3.4 ± 0.9 W
ADP	244 ± 199 µmol/l
$Q_{max,lin}$	0.63 ± 0.34 mmol/l/s
$Q_{max,ADP}$	0.55 ± 0.25 mmol/l/s
V_{PCr}	0.46 ± 0.19 mmol/l/s

[a]One female subject was measured twice.

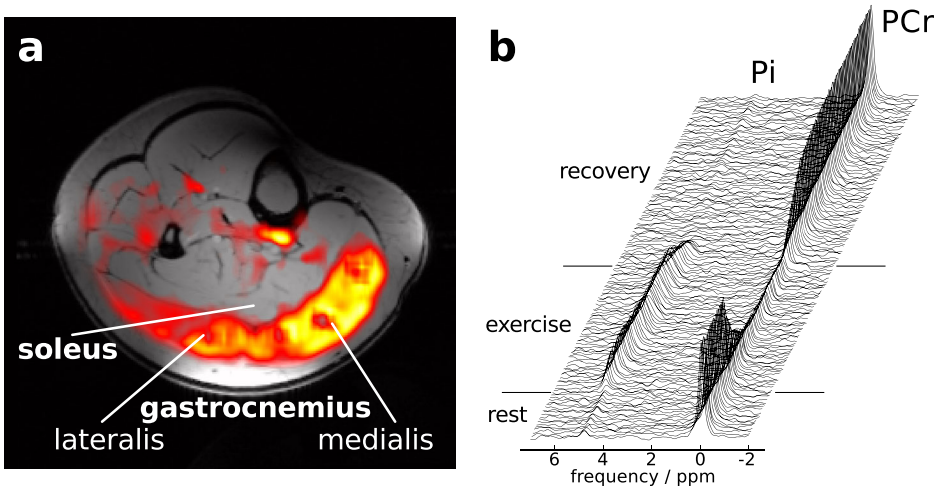

Figure 1. (a) EPI slice of human calf, showing the difference of S_{EPI} during the post exercise peak and the pre exercise intensity, overlaid on an axial gradient-echo image. Zero or negative values are transparent. (b) Time series of unaveraged single-shot ^{31}P spectra (every 6 s) localised to gastrocnemius medialis.

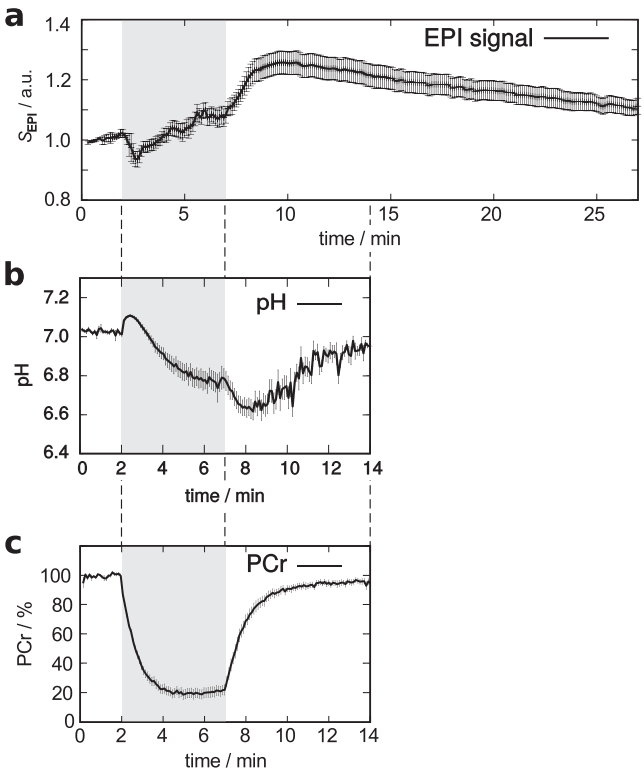

Figure 2. Mean ± standard error of the mean of (a) S_{EPI}, (b) pH and (c) PCr signal time course. Data from the two subjects with very slow PCr recovery and long TTP S_{EPI} were excluded from plots (b and c).

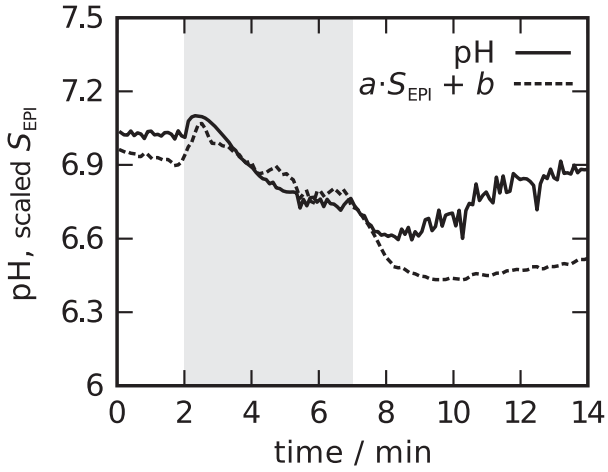

Figure 3. pH(t) and rescaled $S_{EPI}(t)$ time courses, mean over all subjects.

evolution of pH and a linear dependence between $S_{EPI}(t)$ and pH (t) was found (cross-correlation coefficient $r = -0.85 \pm 0.07$) from the onset of exercise until 1 min of initial recovery; see Figure 3.

While exercising, gastrocnemius PCr dropped rapidly and reached a steady state after approximately 3 min of exercise (Fig. 2c). After the end of exercise, PCr recovered (Fig. 2c) to pre exercise levels ($\tau_{PCr\ recovery} = 83 \pm 72$ s). P_i signal dropped faster than PCr increased during recovery (see Table 1); the correlation between the time constants $\tau_{PCr\ recovery}$ and $\tau_{P_i\ recovery}$ was highly significant ($r = 0.98$, $p < 10^{-7}$). The EPI signal increased rapidly after the exercise and reached its maximum after approximately 3 min post exercise (Table 1, Fig. 2a). In contrast to PCr, S_{EPI} did not return completely to pre exercise levels within the duration of the scan (i.e. 27 min).

Recorded force levels were 34 ± 12 % and 38 ± 10 % of individual maximum voluntary contraction force during EPI acquisitions and ^{31}P MRS, respectively, and did not correlate significantly with any of the reported parameters, indicating that the intended normalisation of force was effective. Between the two experiments, no significant difference in mechanical work was observed: the inter-block correlation of work per cross-sectional area was ($r = 0.91$, $p < 10^{-7}$). The metabolic response to exercise, however, measured as end exercise PCr depletion, varied considerably between subjects and ranged from 50 to 98 %. PCr depletion correlated significantly with mechanical work divided by the gastrocnemius medialis' cross-sectional area ($r = 0.50$, $p = 0.02$). This heterogeneity in PCr genetive resulted in a reasonable dynamic range of individual data points (see Figs 2c and 4).

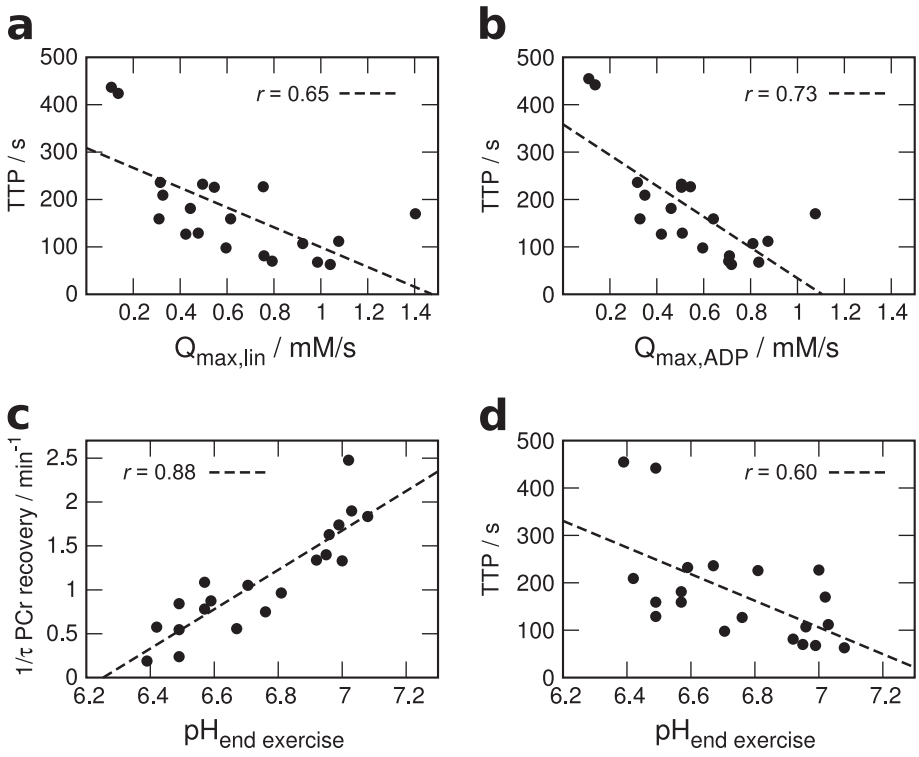

Figure 4. Correlation of TTP S_{EPI} and (a) linear and (b) ADP-driven models of maximum oxidative phosphorylation, along with end exercise pH correlated with both (c) PCr recovery rate $1/\tau$ and (d) TTP S_{EPI}.

Aside from the correlation of pH(t) and $S_{EPI}(t)$, interesting correlations were found between the TTP of the post exercise EPI signal and the time constants of PCr (Fig. 2c) and, likewise, P_i recovery. TTP also correlated highly significantly with other measured parameters listed in Table 2, most importantly with both measures of Q_{max} (Fig. 4a, b). For illustration, the PCr and S_{EPI} during recovery of four subjects are shown in Figure 5. Two volunteers with long (#6 and #7) and two with relatively short (#10 and #21) $\tau_{PCr\ recovery}$ were selected. Subjects with shorter TTP S_{EPI} (Fig. 5a) also had shorter $\tau_{PCr\ recovery}$ (Fig. 5b). Note that the data shown in Figure 5 are not those from the two subjects with extremely slow PCr recovery and TTP S_{EPI} (#5 and #8). No significant correlations with the time to half-peak value, i.e. how fast S_{EPI} returned to baseline, were found.

Also note the correlation between the magnitude of the post exercise T_2^* change (ΔS_{EPI}), defined as peak amplitude minus end exercise S_{EPI}, and both Q_{max} and end exercise pH (see Table 2) when excluding the two subjects (#5 and #8) with PCr depletion greater than 95 %.

In addition, $pH_{end\ exercise}$ correlated with V_{PCr} ($r = 0.75$, $p = 0.0001$), $1/\tau_{PCr\ recovery}$ ($r = 0.86$, $p = 10^{-6}$) and PCr depletion ($r = 0.86$, $p = 10^{-6}$).

DISCUSSION

pH and T_2^* changes

In this study, a strong link between high-energy phosphate and pH kinetics, cellular energy metabolism and the skeletal muscle T_2^* -weighted signal (S_{EPI}) was observed.

The most interesting result is that, during exercise and the first minute of recovery, the time course of S_{EPI} was a linear function of the pH time course (Fig. 3), i.e. cross-correlation analysis showed that pH explained $r^2 = 72\%$ of the variance in S_{EPI}. This result is particularly interesting, given that S_{EPI} and pH were measured in consecutive exercise-recovery blocks and not simultaneously. To our knowledge, this has not been shown with high temporal resolution in human muscle before. For the comparison of ^{31}P MRS and T_2^* weighted S_{EPI}, it was essential to achieve the high temporal resolution of 6 s and accurate localisation of both ^{31}P and ^{1}H data from the same tissue.

Our results confirm earlier findings on the pH dependence of T_2 in healthy volunteers (34) and in frog muscle (35). The underlying mechanism is probably the osmotic pressure change due to intracellular accumulation of metabolites, such as P_i, Cr or

Table 2. Correlation coefficients of TTP S_{EPI} and ΔS_{EPI} with the most important parameters of ^{31}P kinetics and measures of energy metabolism

	$\tau_{PCr\ recovery}$	$\tau_{P_i\ recovery}$	V_{PCr}	$Q_{max,lin}$	$Q_{max,ADP}$	ADP	pH_{endex}
TTP S_{EPI}	0.89[e]	0.89[e]	0.77[d]	0.65[b]	0.73[c]	0.74[c]	0.60[b]
ΔS_{EPI}	0.41	0.41	-0.47[a]	-0.56[b]	-0.56[b]	0.10	-0.57[b]

[a]$p < 0.05$; [b]$p < 0.01$; [c]$p < 0.001$; [d]$< 10^{-4}$; [e]$< 10^{-6}$.

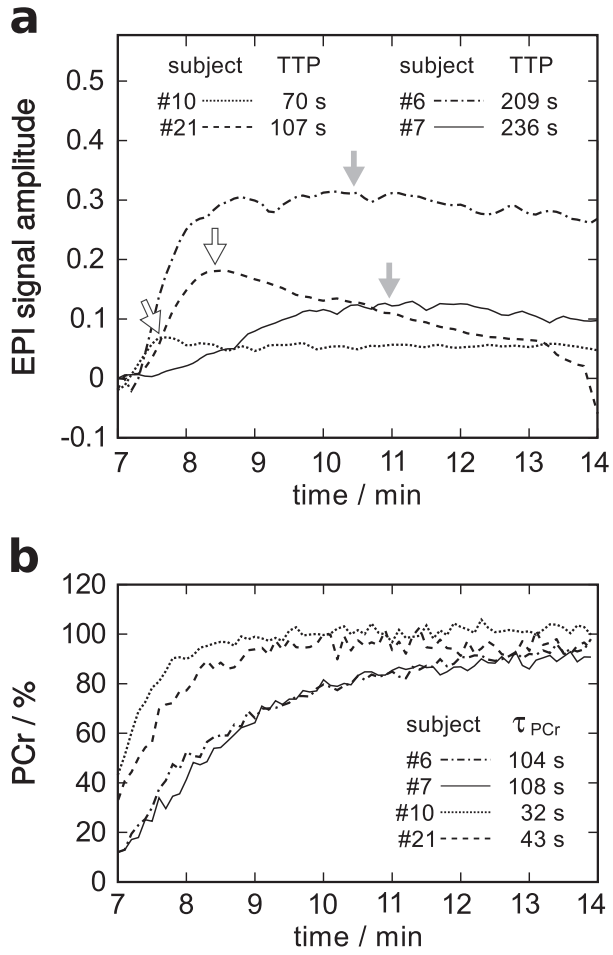

Figure 5. (a) EPI and (b) PCr signal during recovery from exercise of four representative subjects: two with relatively long TTP S_{EPI} and two others with short values, as indicated by the arrows and $\tau_{PCr\ recovery}$, were selected.

lactate, which drives a proton-dependent water shift between intra- and extra-cellular compartments (12).

After around 1 min post exercise, the P_i signal became very small and therefore pH(t) quantification was not very reliable. Nonetheless, it is apparent that the linear relationship of S_{EPI} and pH does not hold any more during later stages of recovery, i.e. pH returns to baseline values much more rapidly than S_{EPI}. This, however, is still consistent with the assumption that T_2^* changes are driven by H^+ levels: when the osmotic gradient across the cellular membrane is lost, only diffusion, which is much slower, remains to restore pre exercise states eventually (2).

Energy metabolism and T_2^* changes

The data presented in this work revealed highly significant correlations of TTP S_{EPI} with both measures of Q_{max}, as well as with $\tau_{PCr\ recovery}$. When plotting the data (Figs 2c, 4, 5), the picture is very consistent: more PCr depletion corresponds to lower end-exercise pH, (Fig. 4a) slower PCr recovery (36) and consequently lower Q_{max} and, in turn, also a longer time to peak of S_{EPI}. A plausible and simple explanation is that faster PCr resynthesis, caused by higher mitochondrial ATP production (Q_{max}) (5), leads to shorter periods of elevated mitochondrial activity and earlier peak acidosis or minimum pH and thus maximum T_2^* and consequently increased EPI signal.

A correlation analysis of PCr and Q_{max} with respect to the amplitude of ΔS_{EPI} resulted in significant correlations similar to those of TTP S_{EPI}, but the correlation coefficients were generally lower.

The actual amount of the contribution of the skeletal muscle BOLD effect to the measured S_{EPI} is hard to determine. Obviously there is an initial drop in T_2^* weighted S_{EPI}, which is not explained by the initial rise in pH; neither is the post exercise S_{EPI} maximum. There is a qualitative difference between T_2 and T_2^* weighted data, in that T_2 apparently increases with the onset of exercise, see for example (13), while T_2^* decreased, which can then be attributed to susceptibility effects such as the BOLD effect. At least in frogs (35), skeletal muscle volume changes were found to be another important contribution to changes in T_2.

Comparison with previous studies

Vandenborne *et al.* (37) used ^{31}P Hadamard spectroscopic imaging before and during exercise and T_2^* mapping before and immediately following exercise, both with relatively low (~1 min) temporal resolution. They found significant correlations of T_2^* with P_i and pH during plantar flexions. In other studies where both ^{31}P MRS and S_{EPI} were acquired in exercising muscle, the rather large volume of interest was defined based on the sensitive volume of a single loop coil (38,39,28). In our previous work (28), studying ischaemic exercise, S_{EPI} and ^{31}P spectroscopy were not measured on the same day. All of the above-mentioned studies were performed at static magnetic field strengths between 2 and 4 T.

To our knowledge, a correlation between TTP S_{EPI} and PCr recovery has so far only been reported by Wary *et al.* (38). In that study, a correlation between TTP S_{EPI} and $\tau_{PCr\ recovery}$ was found only in patients with a glycogen storage disorder and not in healthy volunteers. A possible explanation for the discrepancy from our findings, which show strong correlations also in healthy subjects, could be that an exercise intensity based on a target PCr depletion resulted in a smaller dynamic range of the measured parameters compared with our study. Reported TTP S_{EPI} values were all shorter than 100 s and $\tau_{PCr\ recovery} < 70$ s in the control group, while in this study they ranged up to ~450 and ~300 s, respectively. It should be mentioned that the correlations remain significant even when rejecting these two extreme values. Further differences between this study and the work of Wary *et al.* (38), which could play a role in comparability of the results, are localisation technique, field strength and repetition time used.

In contrast to the strong PCr depletion values measured in this work, a recent study on ^{31}P kinetics in the quadriceps muscles with repeated CSI (40) during knee extension exercise found less PCr depletion, even though subjects claimed to be exhausted. The very slow sampling (4 min) using CSI and the definition of true voxel boundaries, limited by the point-spread function, could be at least partially responsible, as the authors themselves discussed (40). Also, because the quadriceps muscles are much bigger than the gastrocnemius, systemic effects could be more limiting than in our study.

Design and data quality

The ^{31}P data acquired in this study were of high quality in terms of line width, SNR and stability over the duration of the experiment. PCr, P_i and hence also pH were quantified from single

spectra. This applied similarly to T_2^* weighted data, as EPI contained few artefacts even during exercise, with the exception of two subjects whose data were not included in the analysis. In an experiment where motion is an essential feature, more motion-related artefacts would have been expected. Fixation in the form-fitted coil and compliance of the subjects were apparently sufficient in 19 of 21 cases. Good data stability was evident from the fact that image registration was not required. An important contribution to ^{31}P data quality was the use of a form-fitted calf coil array. The bigger sensitive volume and the more homogeneous B_1 transmit field, compared with a planar loop coil, allowed for voxel placement optimised to the protocol and not limited by the sensitive volume of the coil. The model for the post exercise S_{EPI} response fitted the present data as well as previously shown ischaemia-reperfusion data (29).

The authors are aware of the fact that systematic effects of repeated exercise potentially influenced the results and the study design could be improved, but technical limitations and practical considerations, in particular subject compliance and scan time, were considered more important. The excellent agreement between S_{EPI} and pH time courses is a strong indicator that no systematic errors were caused by the protocol. No significant differences in muscle force or mechanical workload between the two measurement blocks were found. The observed heterogeneity in PCr depletion and hence a sufficient dynamic range in the measured parameters allowed for a meaningful correlation analysis even in healthy young volunteers.

^{31}P data were acquired for 14 min, based on the expected recovery times from the literature (2,4) and previous studies from our lab. $\tau_{PCr\ recovery}$ and depletions reported in this study correspond to a PCr resynthesis of >99 % after 7 min of recovery. On average, pH had not fully recovered to baseline values; however the correlation to S_{EPI}, reported here, ended much earlier.

^{31}P data acquisition was specifically localised to the gastrocnemius medialis muscle. Signals from other tissues, particularly the less working soleus muscle (21), do not contribute, because the contamination from outside the selected VOI with the semi-LASER sequence used was shown to be as low as 1 % (21). Due to *J*-evolution, the ATP signal was too low for reliable quantification; therefore, resting PCr and ATP concentrations were assumed. Figure 1a clearly supports the hypothesis that the main workload was carried by the gastrocnemius muscles only, confirming the validity of the locations of ^{31}P MRS voxels and ^{1}H MRI ROIs.

Acquiring EPI imaging with long repetition delay and hence low sensitivity to T_1 and inflow effects was an important design feature, allowing us to focus on T_2^* weighting. Actual dynamic T_2^* and T_2 parameter mapping would be the next step to investigate.

CONCLUSIONS

A direct link between mitochondrial function, cellular energy metabolism, acid-base equilibrium and T_2^* was found during exercise and recovery. In particular, pH time courses apparently induce the observed T_2^* weighted signal time course.

The combination of time-resolved localised ^{31}P spectroscopy and T_2^* sensitive MRI revealed highly significant correlations between the time constant of PCr resynthesis, the rate of oxidative phosphorylation and the time to peak of the post exercise S_{EPI} response. In our opinion, ^{31}P studies on exercising muscles benefit significantly from accurate localisation schemes, particularly when conclusions are drawn from comparisons with other localised methods, such as e.g. MR imaging.

This work is an important contribution to the interpretation of the skeletal muscle functional MRI (S_{EPI}) signal. This is of particular importance when studying pathologies such as diabetes mellitus, where impaired muscle metabolism is known to play an important role in the development of insulin sensitivity and cardiovascular complications are common.

Acknowledgements

This work was financially supported by the Austrian BMWFJ FFG Project Nr. 832107, 'Research Studio for High Field MR Components' and The Austrian Science Fund (FWF) Project Nr. J 3031-N20.

REFERENCES

1. Perry CG, Kane DA, Lanza IR, Neufer PD. Methods for assessing mitochondrial function in diabetes. Diabetes 2013; 62: 1041–1053.
2. Prompers JJ, Jeneson JA, Drost MR, Oomens CC, Strijkers GJ, Nicolay K. Dynamic MRS and MRI of skeletal muscle function and biomechanics. NMR Biomed. 2006; 19: 927–953.
3. Damon BM, Wadington MC, Hornberger JL, Lansdown DA. Absolute and relative contributions of BOLD effects to the muscle functional MRI signal intensity time course: effect of exercise intensity. Magn. Reson. Med. 2007; 58: 335–345.
4. Chance B, Im J, Nioka S, Kushmerick M. Skeletal muscle energetics with PNMR: personal views and historic perspectives. NMR Biomed. 2006; 19: 904–926.
5. Kemp GJ, Radda GK. Quantitative interpretation of bioenergetic data from ^{31}P and ^{1}H magnetic resonance spectroscopic studies of skeletal muscle: an analytical review. Magn. Reson. Q. 1994; 10: 43–63.
6. Radda GK. Control of energy metabolism during muscle contraction. Diabetes 1996; 45(Suppl 1): 88–92.
7. Schmid AI, Schrauwen-Hinderling VB, Andreas M, Wolzt M, Moser E, Roden M. Comparison of measuring energy metabolism by different ^{31}P-magnetic resonance spectroscopy techniques in resting, ischemic, and exercising muscle. Magn. Reson. Med. 2012; 67: 898–905.
8. Kemp GJ, Roussel M, Bendahan D, Fur YL, Cozzone PJ. Interrelations of ATP synthesis and proton handling in ischaemically exercising human forearm muscle studied by ^{31}P magnetic resonance spectroscopy. J. Physiol. 2001; 535: 901–928.
9. Layec G, Haseler LJ, Trinity JD, Hart CR, Liu X, LeFur Y, Jeong EK, Richardson RS. Mitochondrial function and increased convective O_2 transport: Implications for the assessment of mitochondrial respiration in vivo. J. Appl. Physiol. 2013; 115: 803–811.
10. Cea G, Bendahan D, Manners D, Hilton-Jones D, Lodi R, Styles P, Taylor DJ. Reduced oxidative phosphorylation and proton efflux suggest reduced capillary blood supply in skeletal muscle of patients with dermatomyositis and polymyositis: a quantitative ^{31}P-magnetic resonance spectroscopy and MRI study. Brain 2002; 125: 1635–1645.
11. Carlier PG, Bertoldi D, Baligand C, Wary C, Fromes Y. Muscle blood flow and oxygenation measured by NMR imaging and spectroscopy. NMR Biomed. 2006; 19: 954–967.
12. Meyer RA, Prior BM. Functional magnetic resonance imaging of muscle. Exerc. Sport Sci. Rev. 2000; 28: 89–92.
13. Damon BM, Hornberger JL, Wadington MC, Lansdown DA, Kent-Braun JA. Dual gradient-echo MRI of post-contraction changes in skeletal muscle blood volume and oxygenation. Magn. Reson. Med. 2007; 57: 670–679.
14. Fleckenstein AL, Canby RC, Parkey RW, Peshock RM. Accute effects of exercise on MR imaging of skeletal muscle in normal volunteers. Am. J. Roentgenol. 1988; 151: 271–237.
15. Noseworthy MD, Bulte DP, Alfonsi J. BOLD magnetic resonance imaging of skeletal muscle. Semin. Musculoskelet. Radiol. 2003; 7: 307–315.
16. Meyer RA, Towse TF, Reid RW, Jayaraman RC, Wiseman RW, McCully KK. BOLD MRI mapping of transient hyperemia in skeletal muscle after single contractions. NMR Biomed. 2004; 17: 392–398.
17. Jacobi B, Bongartz G, Partovi S, Schulte AC, Aschwanden M, Lumsden AB, Davies MG, Loebe M, Noon GP, Karimi S, Lyo JK, Staub D, Huegli RW, Bilecen D. Skeletal muscle BOLD MRI: from underlying

physiological concepts to its usefulness in clinical conditions. J. Magn. Reson. Imaging 2012; 35: 1253–1265.
18. Schewzow K, Andreas M, Moser E, Wolzt M, Schmid AI. Automatic model-based analysis of skeletal muscle BOLD-MRI in reactive hyperemia. J. Magn. Reson. Imaging 2013; 38: 963–969.
19. Moser E, Stahlberg F, Ladd ME, Trattnig S. 7-T MR – from research to clinical applications? NMR Biomed. 2012; 25: 695–716.
20. Laistler E, Goluch S, Kuehne A, Meyerspeer M, Schmid AI, Sieg J, Herrmann T, Mallow J, Bernarding J, Moser E. A form-fitted 3 channel ^{31}P, two channel ^{1}H transceive coil for calf muscle studies at 7 T. In *Proceedings of the 21st Annual Meeting ISMRM*. 2013; 2782.
21. Meyerspeer M, Scheenen T, Schmid AI, Mandl T, Unger E, Moser E. Semi-LASER localized dynamic ^{31}P magnetic resonance spectroscopy in exercising muscle at ultra-high magnetic field. Magn. Reson. Med. 2011; 65: 1207–1215.
22. Scheenen TW, Heerschap A, Klomp DW. Towards ^{1}H-MRSI of the human brain at 7 T with slice-selective adiabatic refocusing pulses. MAGMA 2008; 21: 95–101.
23. Fiedler GB, Schmid AI, Goluch S, Moser E, Meyerspeer M. Signal-to-noise ratio analysis of ^{31}P MRS in skeletal muscle: Influence of localization schemes, RF coils and field strength. In *Proceedings of the 21st Annual Meeting ISMRM*. 2013; 1971.
24. Wary C, Naulet T, Thibaud JL, Monnet A, Blot S, Carlier PG. Splitting of Pi and other ^{31}P NMR anomalies of skeletal muscle metabolites in canine muscular dystrophy. NMR Biomed. 2012; 25: 1160–1169.
25. Kan HE, Klomp DW, Wong CS, Boer VO, Webb AG, Luijten PR, Jeneson JA. In vivo ^{31}P MRS detection of an alkaline inorganic phosphate pool with short T_1 in human resting skeletal muscle. NMR Biomed. 2010; 23: 995–1000.
26. Meyerspeer M, Robinson S, Nabuurs CI, Scheenen T, Schoisengeier A, Unger E, Kemp GJ, Moser E. Comparing localized and nonlocalized dynamic ^{31}P magnetic resonance spectroscopy in exercising muscle at 7 T. Magn. Reson. Med. 2012; 68: 1713–1723.
27. Moser E. Ultra-high-field magnetic resonance: Why and when? World J. Radiol. 2010; 2: 37–40.
28. Andreas M, Schmid AI, Keilani M, Doberer D, Bartko J, Crevenna R, Moser E, Wolzt M. Effect of ischemic preconditioning in skeletal muscle measured by functional magnetic resonance imaging and spectroscopy: a randomized crossover trial. J. Cardiovasc. Magn. Reson. 2011; 13: 32–32.
29. Andreas M, Schmid AI, Doberer D, Schewzow K, Weisshaar S, Heinze G, Bilban M, Moser E, Wolzt M. Heme arginate improves reperfusion patterns after ischemia: a randomized, placebo-controlled trial in healthy male subjects. J. Cardiovasc. Magn. Reson. 2012; 14: 55–55.
30. Vanhamme L, vanden Boogaart A, van Huffel S. Improved method for accurate and efficient quantification of MRS data with use of prior knowledge. J. Magn. Res. 1997; 129: 35–43.
31. Naressi A, Couturier C, Devos JM, Janssen M, Mangeat C, de Beer R, Graveron-Demilly D. Java-based graphical user interface for the MRUI quantitation package. Magn. Reson. Mater. Phys. 2001; 12: 141–152.
32. Kemp GJ, Meyerspeer M, Moser E. Absolute quantification of phosphorus metabolite concentrations in human muscle in vivo by ^{31}P MRS: a quantitative review. NMR Biomed. 2007; 20: 555–565.
33. Taylor DJ, Styles P, Matthews PM, Arnold DA, Gadian DG, Bore P, Radda GK. Energetics of human muscle: exercise-induced ATP depletion. Magn. Reson. Med. 1986; 3: 44–54.
34. Cheng HA, Robergs RA, Letellier JP, Caprihan A, Icenogle MV, Haseler LJ. Changes in muscle proton transverse relaxation times and acidosis during exercise and recovery. J. Appl. Physiol. 1995; 79: 1370–1378.
35. Damon BM, Gregory CD, Hall KL, Stark HJ, Gulani V, Dawson MJ. Intracellular acidification and volume increases explain R_2 decreases in exercising muscle. Magn. Reson. Med. 2002; 47: 14–23.
36. Iotti S, Lodi R, Frassineti C, Zaniol P, Barbiroli B. In vivo assessment of mitochondrial functionality in human gastrocnemius muscle by ^{31}P MRS. The role of pH in the evaluation of phosphocreatine and inorganic phosphate recoveries from exercise. NMR Biomed. 1993; 6: 248–253.
37. Vandenborne K, Walter G, Ploutz-Snyder L, Dudley G, Elliott MA, Meirleir KD. Relationship between muscle T–2^* relaxation properties and metabolic state: a combined localized ^{31}P-spectroscopy and ^{1}H-imaging study. Eur J. Appl. Physiol. 2000; 82: 76–82.
38. Wary C, Nadaj-Pakleza A, Laforêt P, Claeys KG, Carlier R, Monnet A, Fleury S, Baligand C, Eymard B, Labrune P, Carlier PG. Investigating glycogenosis type III patients with multi-parametric functional NMR imaging and spectroscopy. Neuromuscul. Disord. 2010; 20: 548–558.
39. Wray DW, Nishiyama SK, Monnet A, Wary C, Duteil S, Carlier PG, Richardson RS. Multiparametric NMR-based assessment of skeletal muscle perfusion and metabolism during exercise in elderly persons: preliminary findings. J. Gerontol. A. Biol. Sci. Med. Sci. 2009; 64: 968–974.
40. Cannon DT, Howe FA, Whipp BJ, Ward SA, McIntyre DJ, Ladroue C, Griffiths JR, Kemp GJ, Rossiter HB. Muscle metabolism and activation heterogeneity by combined ^{31}P chemical shift and T_2 imaging, and pulmonary O_2 uptake during incremental knee-extensor exercise. J. Appl. Physiol. 2013; 115: 839–849.

